Antimicrobial properties of nanostructured surfaces – demonstrating the need for a standard testing methodology

Martyna Michalska,*[a†] Ralu Divan,[b] Philippe Noirot[a] and Philip D. Laible[a]

[a]Biosciences Division, Argonne National Laboratory, Argonne, IL 60439, USA. E-mail: m.michalska@ucl.ac.uk
[b]Center for Nanoscale Materials, Argonne National Laboratory, Argonne, IL 60439, USA.
†Current address: Photonic Innovations Lab, Department of Electronic and Electrical Engineering, University College London, London, WC1E 7JE, UK

Abstract: Bioinspired nanostructured materials that exhibit antimicrobial properties are being synthesized and tested at increasing rates for use in healthcare, manufacturing processes, and diagnostics. Although progress has been made in improving and understanding their bactericidal activity, arguably, the biggest problem currently in the field is the lack of a standard testing methodology that allows for optimal characterization and better comparison of emerging nanostructures. Here, we examine two forms of nanostructured silicon that vary in their ability to kill certain bacterial species due to different physical mechanisms and derive guidelines for the comparative testing. We perform a comprehensive evaluation of methodologies used extensively in the field (e.g., colony counting and live dead analysis) and the novel application of high-throughput flow cytometry. The data reveal how the techniques are complementary but not always directly equivalent or correlative. Therefore, comparison of results obtained using different methodologies on different materials can be grossly misleading. We report significant variations in bactericidal efficiencies depending on experimental environments (medium type, etc.) and methodologies employed. In addition, we demonstrate how cytometry is yet another powerful complementary tool that can aid the mechanistic understanding of antimicrobial activities of rough surfaces. Besides standardization for comparison, ultimately, evaluation methods need to consider anticipated applications. Then and only then can the true potential (or limitation) of a novel material be determined for its suitability for advancement in a particular field of use.

Introduction

Bacteria tend to colonize most surfaces, often forming biofilms – organized communities that have the ability to withstand treatment by conventional antiseptic agents.[1] This tendency is not only a potential threat in healthcare environments leading to, e.g., implant-associated infections, but also in areas such as food-related industries, water purification systems, and bathroom surfaces.[2–6] Multi-drug resistance is yet another alarming problem, with more than 2.8 million people in the U.S. suffering from infections caused by multi-drug-resistant bacteria each year.[7] Therefore, there is a pressing need for new strategies to combat bacterial colonization which will be safe, sustainable, and ideally, will not induce antimicrobial resistance.

To address these challenges, bioinspired nanostructured materials and coatings that repel (antifouling) and/or mechanically kill bacteria upon contact through physical forces (mechano-bactericidal) have been widely investigated.[6,8–14] The mechano-bactericidal surfaces possess high-aspect-ratio nanoprotrusions (pillars, wires, cones), capable of inducing stress onto the bacterial envelope, ultimately leading to its disruption.[15–18] Depending on the geometry of nanoprotrusions (pitch, shape, height), the surfaces are able to lyse bacterial cells *via* different physical mechanisms, varying in the rates of killing and in the range of organisms affected (spectrum of activity).[18–24] Alternatively, the roughness of a surface may greatly alter its wetting properties, affecting or preventing cell adhesion leading to the ability of surfaces to self-clean.[25–27] In contrast to chemical approaches in which a dose of a bactericidal agent is finite, these new surfaces have the potential for more sustained bactericidal activities. Recently, it has been pointed out that the innovation and commercialization of new products has been greatly hindered by lack of (i) standardization in testing of new antimicrobial surfaces and (ii) consideration of differences in antimicrobial mechanisms by existing industrial standard methodologies.[2,28–30] An excellent and extensive list of the most common, currently in use, methods to evaluate such antimicrobial designs has been provided by Sjollema *et al*.[31] Based on the antimicrobial mechanism, various methods are recommended for testing designs which act through (i) a release of an antimicrobial agent, (ii) contact-killing, or (iii) cell-repelling properties. Importantly, emerging

antimicrobial nanostructures form a new class that requires a revision of current methodologies as recently articulated by Senevirathne *et al.*[30] It is noteworthy that the term *antimicrobial* refers to activity against microorganisms including bacteria, fungi, protozoa and microalgae whereas the terms *antibacterial* and *bactericidal* refer more specifically to activity against bacteria.

In general, contact-killing surfaces exhibit dense cationic charge responsible for disrupting bacterial cells.[32] Although the nanostructured surfaces do not share the same characteristic, they also eliminate bacteria upon contact and thus, it seems appropriate to evaluate them correspondingly. In this regard, adhesion-based assays – either static (passive) or dynamic where a flow chamber is part of the experimental setup – are generally well suited to characterize contact-killing surfaces where intimate contact between bacteria and tested surfaces is required.[33] For this reason, suspension methods are generally not recommended.[31] Within adhesion-based assays, the surfaces are inoculated with cells, incubated, and rinsed to wash off the non- and loosely-attached cells, which are analyzed for viability. Next, dislodging of attached cells is performed (typically by sonication), and their viability is also assessed. A typical incubation time is up to 24 h as opposed to biofilm-based methods which are longer and must involve presence of nutrients to allow biofilm growth.[31] Although the nanostructured surfaces can be readily subjected to the adhesion-based methods, they differ from the existing contact-killing designs, and thus require additional considerations. For example, as recently highlighted, a presence of external forces such as moving air-liquid interface can impact the quantification of antimicrobial properties of nanostructures.[34] In this vein, an ambiguity around the rinsing step and its impact has been also reported.[30] Furthermore, evaluation of viability of cells attached onto nanostructured surfaces by their dislodging is nearly impossible as the cells are impaled by nanoprotrusions. Consequently, characterizing activity of those surfaces requires novel approaches that consider viability of cells that are both unattached and attached onto the surface.

Assessment of viability, on the other hand, can be complex and often depends on the assay used.[35–37] Typical viability assays employed in the field of bioinspired nanostructures include: spread-plate colony counts, optical density monitoring, live/dead fluorescent staining (fluorescent microscopy), and electron microscopy.[38] It is noteworthy that most assessments are widely available but none offer high throughput. Generally, all techniques show advantages and disadvantages in some areas (Table S1), stressing the importance of using multiple techniques to validate results.

Previously, we identified two distinct bactericidal mechanisms for nanostructured materials that either possess (i) dense and blunt pillars that stretch and tear bacteria attached onto them or (ii) sparse and sharp pillars which directly impale bacterial cells.[18] In this work, we evaluate and compare antibacterial properties of those characteristic surfaces using an adhesion-based method and various viability assays. Additionally, for the first time in this field, we present the use of flow cytometry as an excellent, alternative to the conventional colony counting tool, capable of high-throughput screening of new material designs. We show which methods are complementary, duplicative and/or orthogonal. We also demonstrate how cytometry is yet another powerful technique that can contribute to a mechanistic understanding of the antimicrobial properties of rough surfaces.
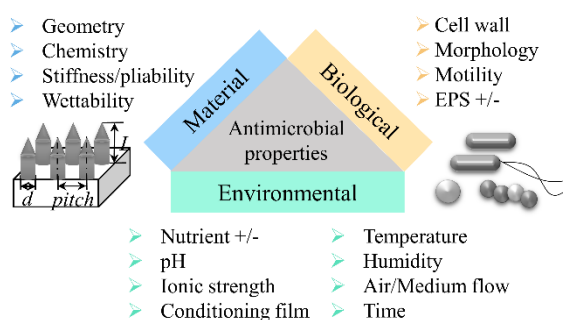

Fig. 1 Variable interacting factors that influence antibacterial activities. Material, environmental, and biological factors all contribute to, and impact the success or failure of the approach to determine antibacterial properties of nanostructured surfaces. *EPS* – extracellular polymeric substance which is a matrix that surrounds cells within the biofilm. *Conditioning film* refers to layers of organic and mineral molecules adsorbed onto the surface upon immersion in a solution that mediates/influences the interaction between the surface and the attached bacteria.

Such properties are a resultant of interacting elements that include material, biological and – importantly but least studied – environmental factors (Fig. 1). In terms of the material performance,

topographical features have been identified as a key surface factor.[39] Recently, material pliability has also been reported as a driving force impacting the performance in some instances.[19] With regards to the biological input, this is mostly driven by differences between Gram-negative and Gram-positive species in mechanical properties of bacterial cell walls, and their motility.[40] Here, we additionally report significant variations in bactericidal efficiencies depending on experimental environments such as medium type, previously noticed[41] but rarely discussed. Overall, this report makes suggestions, brings attention to, and calls for a discussion about the standardization of measurements of antimicrobial properties of nanostructured surfaces to facilitate their rapid deployment.

Results and discussion

Fabrication and characterization of nanostructured surfaces

The killing efficiency of nanostructured surfaces and the spectrum of activity depend on the geometry of the nanopillars (tip shape/size, pitch, and aspect ratio); strongly linked to their bactericidal mechanism.[6] Although some ambiguity remains around the exact mechanism, two scenarios are widely recognized: (i) stretch-and-rupture,[18,42] and (ii) fast piercing by sharp tips.[18,21,43] Simply put, after adhesion, the cellular envelopes stretch and tear on nanopillars with blunt and relatively wide tips, whereas cells are directly pierced by nanopillars that possess sharp tips. Therefore, both patterns were chosen to serve as experimental examples of the two mechanisms. It is noteworthy that enhanced stretching can be gained not only by manipulating the tip shape and pitch but also the aspect ratio by means of an energy storage-release mechanism, as recently reported by Ivanova *et al.*[17]
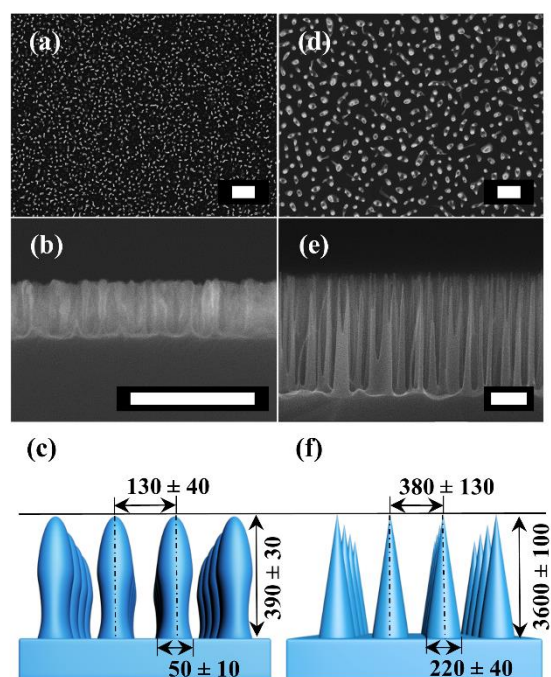

Fig. 2 Topographical features of nanostructured silicon surfaces: (a-c) blunt, and (d-f) sharp nanopillars. SEM micrographs present top views (upper panel) and cross sections (middle panel). Scale bar 1 μm. (c, f) Schematics depicting nanopillar morphologies with characteristic dimensions (scales are not conserved).

Nanostructured silicon surfaces with various topographical features were fabricated by lithography-free reactive ion etching using O_2/SF_6 plasma. After 90 seconds of etching, the resulting nanopillars were 390 nm tall and possessed wide, blunt tips (Fig. 2a-c). As the etching proceeded, nearly ten times taller pillars evolved (3.6 μm) with sharp, narrow tips, and sparser distribution (4 pillars per μm^2 in respect to 26 per μm^2; Fig. 2d-f). The patterns were fairly homogenous and did not show any hierarchical order. Due to the high roughness, both samples exhibit superhydrophilic character (water contact angles below <10°), in which water spreads instantly across the surface.

Evaluation of antibacterial properties of nanostructured surfaces

To assess the antibacterial properties of the resulting nanostructures, we employed an adhesion-based static method schematically depicted in Fig. 3. The protocol follows the principles of the ISO standard (International Organization for Standardization) JIS Z 2801 (2010),[44] currently in use to test surfaces of antibacterial products of plastics, metals, ceramics, etc., with certain modifications. Bacteria suspended in a small volume (tens of µl) are placed on test and control surfaces (of reduced size in respect to the standard, see Materials and Methods) for a period of time, and subsequently the surfaces are rinsed to remove non-adhering cells. The viability of non-adhering cells and those attached on the surface is determined. Here, the latter analysis expands beyond the recommendations given by the standard, which is however necessary to elucidate the origin of reduction in the number of viable cells by the tested design compared to a control smooth surface (Fig. 3b). Lack of such analysis, otherwise, raises the question whether the surface solely favors bacterial adhesion and allows them to proliferate, or instead, is capable of inducing killing. Additionally, the standard assumes all the bacteria are dislodged from the surface, which does not apply to nanostructured surfaces, further requiring the double approach.
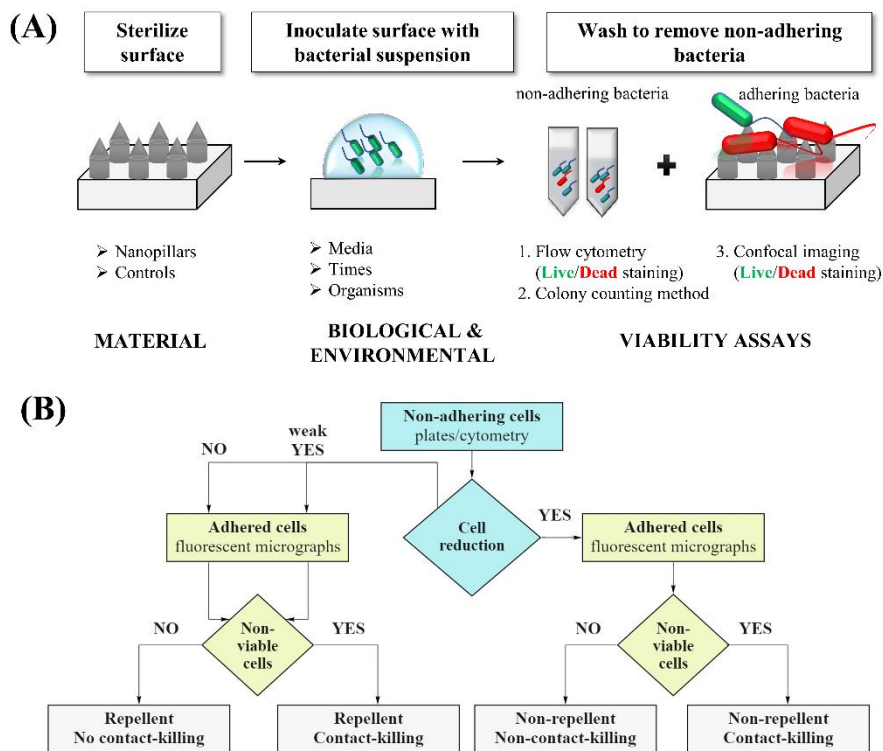

Fig. 3 (a) Schematic of adhesion-based method used to evaluate antimicrobial properties of nanostructured surfaces. Various material, biological and environmental conditions were chosen (nanopatterns, bacterial species and media, respectively). First, the sterilized surfaces to be tested and appropriate controls are inoculated with a droplet containing bacteria in a given medium. After incubation time, the surface is gently washed to retrieve non-adhering bacteria and their viability is assayed using flow cytometry (1) and colony counting (2) methods. The surface with adhering bacteria is further imaged using confocal microscopy (3), and viable and non-viable cells are counted. (b) Flow diagram for testing and results interpretation. The decision tree clearly shows why both types of samples (retrieved cells = non-adhering, blue box; and adhered onto the surface, yellow box) are needed to evaluate mechanism of action of nanostructured surfaces in terms of: (a) their ability to repel (repellent or non-repellent), and (b) their ability to kill (mechano-bactericidal activity; contact-killing or non-contact-killing).

Figure 3b broadly illustrates a decision tree for testing and interpretation of the mechanism of action of nanostructured surfaces, further highlighting the importance to study both the retrieved cells (non-adhering, blue box) and the cells adhered onto the surface (yellow box). Having information from both adhered and non-adhering cells will allow for stronger conclusions on surface properties in terms of: (a) their ability to repel (decisive classification of repellent or non-repellent), and (b) their ability to kill (additional information on mechano-bactericidal activity, including categorization as contact-killing or non-contact-killing). Note, additional information can be derived from these expanded sets of information based on overall number of adhered cells, which may speak to the rate of killing and ability of cell lysis. As a prime example, if not many cells are present on the surface, the materials may have caused their complete disintegration, and thus rendered them impossible to visualize by fluorescent micrographs. Here, SEM imaging could aid interpretation of the results, for instance. It should also be

noted that if the surface proves repellent, a further examination by flow perfusion methods is advised, as they better allow to control mass transport.[31]

The highly hydrophilic character of the sample, on the other hand, necessitates the inoculation volume to be reduced so that spilling of the sample over the edges can be prevented. While the volume is reduced, one should mind to concentrate the inoculum to reach the anticipated challenge numbers – a number of microorganisms used to challenge the antimicrobial coatings to evaluate their efficacy. The immersion experiments in a bigger volume, on the other hand, could help with prevention of drying out when materials are to be challenged over an extended period of time (e.g., biofilm studies). It is anticipated that bactericidal efficiency expressed by viability of attached cells could be directly compared between adhesion and immersion methods (perhaps if the volume is not excessive, to be determined). However, a reduction in the number of non-adhering cells is not straightforward to compare, as a smaller volume will favor more interactions with the surface. For the samples which exhibit hydrophobic properties, a thin sterile film (e.g.; Parafilm® or glass cover slip) can be employed to facilitate spread of the liquid over the entire surface whilst assuring intimate contact between the surface and the cells.

Two Gram-negative bacteria were used, *Escherichia (E.) coli* and *Rhodobacter (R.) capsulatus*, as they previously displayed marked variations in the response to the surface topographies.[18] Note that although both species are classified as Gram-negative bacteria, *E. coli* and *R. capsulatus* are vastly different is terms of genome content, the ecological niches they evolved in (mammal gut and aquatic environment, respectively), and their metabolic capabilities. The inoculum concentration was adjusted to 10^7 colony forming units (cfu)/ml to allow a sufficient number of adhesion events (visualized by microscopy) within the few-hour experimental plan. However, both the challenge number and bacterial species should be selected according to the intended applications. For example, 2.5×10^6 cfu/ml in JIS Z 2801 corresponds to the concentration of bacteria typically found in patients with a catheter-associated-infections (10^5-10^8 cfu/ml). However, the challenge number could be lowered drastically if the surface is designed to act prophylactically, as it is therefore assumed to interact with lower numbers of cells to begin with. Choice of *E. coli* and *Staphylococcus spp.* is frequently advised by various standards as they represent models for Gram-negative and Gram-positive species, respectively, as well as they constitute major causes of biomaterial-associated infections.[31,44] If the material is to be used in medical applications, fresh clinical isolates are also recommended as repeated culturing may alter the virulence or ability of a strain to form biofilms.[45]
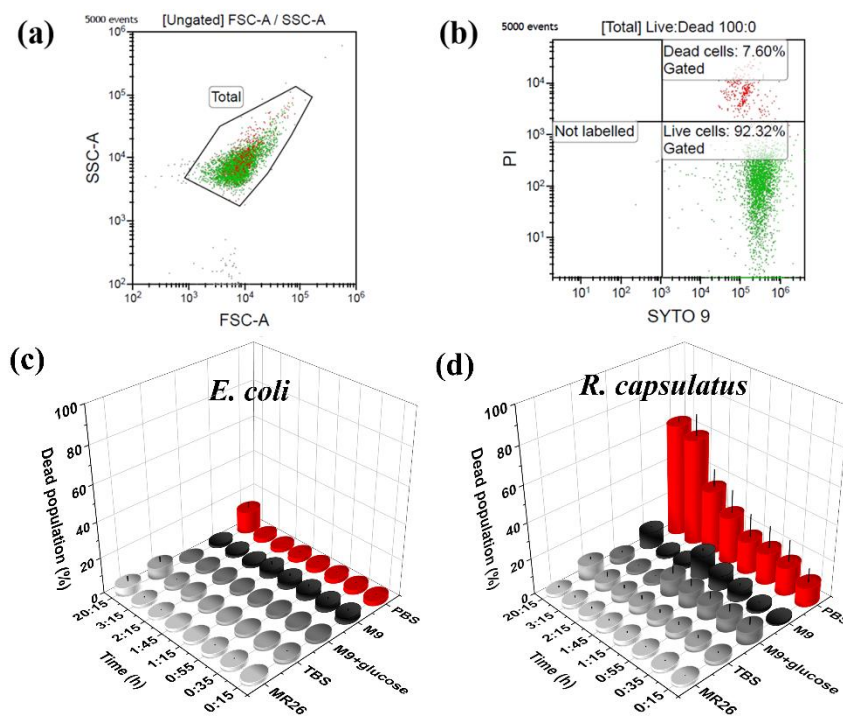

Fig. 4 The impact of medium on susceptibility of (a-c) *E. coli* and (d) *R. capsulatus* cells. Bacteria were suspended in either minimal media (MR26,[52] M9+glucose) or nutrient-free buffers (M9 (salts), PBS, TBS). At certain time intervals, cell suspensions were stained with a live/dead viability kit and assayed by flow cytometry. Numbers of live and dead cells were determined. (a-b) Representative cytograms (dot plots) showing: (a) a cell population of interest within a gate (Total), and (b) live and dead cell populations (green and red, respectively). (c-d) The graphs present temporal evolution of the number of dead cells (*E. Coli* (c) and *R. capsulatus* (d)), expressed as a percentage of the total cell population, for the tested media.

Prior to the evaluation of surface antibacterial activities, we determined the influence of commonly used minimal media and buffers on cell susceptibility by using live/dead fluorescent staining and flow cytometry (Fig. 4). As opposed to the colony counting method, flow cytometry allows for a rapid, high-throughput, and nearly real-time discrimination between viable and non-viable cells based on the viability criteria, predetermined by the choice of fluorescent dyes (Table 1). Here, the cells with compromised membrane are scored as dead (or dying). The staining protocol and cytometer operational conditions have been carefully optimized to yield the most accurate quantitative analysis (Fig. S1-3). Figure 4 shows representative cytograms where a population of interest is first chosen (Fig. 4a), followed by gating out of live and dead sub-groups (Fig. 4b).

The temporal evolution of numbers of non-viable *E. coli* cells indicates a great compatibility with all the media and buffers tested, as the values remained constant and so did the total number of cells (Fig. 4c; Table S4). In contrast, *Rhodobacter* cells exhibited poor survival when suspended in phosphate-buffered saline (PBS) buffer, which is frequently used in biological studies and advised by ISO standard (Table S4). Non-viable cells accumulated over time and the total number of cells dramatically decreased. A weaker susceptibility of *Rhodobacter* cells to M9 salts was also observed (Table S4). The strong susceptibility of *Rhodobacter* to PBS likely involves multiple biological factors that are currently under investigation. Therefore, Tris-buffered saline (TBS) buffer was selected for *Rhodobacter* studies, and both species were eventually investigated in (i) nutrient-rich medium and (ii) an appropriate nutrient-free buffer. Whereas the former media could allow cell growth if long enough time is provided, the latter media do not, allowing a comparison between species that require different culture conditions.

Table 1 A comparison of colony counting and flow cytometry methods used to evaluate antimicrobial properties of nanostructured surfaces.

Characteristics	Colony counting method	Flow cytometry
Time required	Days (sometimes many)	Minutes
Throughput	Low	High
Viability criterion	Ability to form a colony	Dependent on fluorescent probe; multiple available
Quantitative data captured	Viable cells	Viable and non-viable (if dislodged from the surface); debris

It is noteworthy that depending on the deployment setting, material surface chemistry may undergo a gradual change owing to the adsorption of various molecules (minerals, proteins, etc.) upon exposure to body fluids or water of various origin. This phenomenon is called conditioning film formation which may also affect the material performance as adsorption of macromolecules proceeds faster that bacterial adhesion. For example, a number of pathogens exhibit receptors which recognize blood-borne proteins which may enhance adhesion.[46] Such films can also form during the testing of antimicrobial properties if inoculum is suspended in a medium supporting cell growth/proliferation. Thus, if an envisioned application involves conditioning film formation, a surface pre-treatment should be included.[31] Similarly, bacterial cells respond dynamically to the environmental settings which may also change their surface chemistry and turgor pressure, thus impacting their interactions with nanopillars. Furthermore, it has been reported recently that cellular movement in the direction of nutrients accelerates cell adhesion behavior.[47] Besides, dynamic conditions and different shear stress will further affect cell behavior, which is important to consider when challenging a material designed to be deployed under dynamic settings (e.g., catheters, marine coatings etc.).[30,34] Overall, this shows the importance of environmental factors contributing to the interplay between bacterial cells and materials.

Nanostructures with blunt pillars

Having established the testing conditions, we first focus on cell interactions with the blunt pillars (initially studying 2 h incubations). The non-attached bacteria were split into two aliquots. One aliquot was immediately stained and assayed by means of flow cytometry providing real-time data (Fig. 5); and the other aliquot was plated and incubated for 18 h for counting of colony forming units. The images of the attached cells were acquired in parallel complementing the results, thus providing a fuller overview of the sample's performance. Surprisingly, there was no significant increase in the number of retrieved dead cells for the tested nanostructures for both species in respect to the controls (see the cell concentrations in Fig. 5 and Fig. S5). This suggests that both live and dead cells adhere to the surface, as indicated in confocal image for *R. capsulatus,* for instance. Therefore, the concentration of live cells was utilized to determine bactericidal efficiencies that were subsequently compared to the values resulting from colony counting, under various experimental conditions including either rich medium or nutrient-free buffer (Fig. 6).

In the case of *R. capsulatus,* all three methods are duplicative and there is no significant environmental impact observed (Fig. 6b). In contrast, assays with *E. coli* revealed significant differences between both
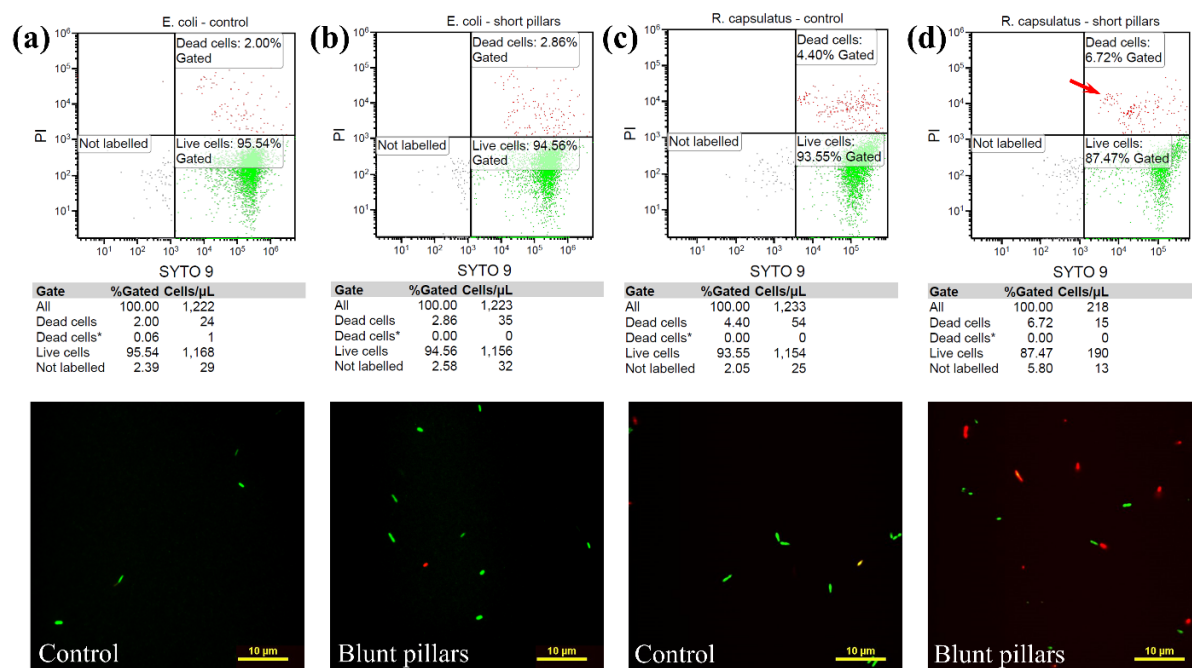

Gate	%Gated	Cells/µL
All	100.00	1,222
Dead cells	2.00	24
Dead cells*	0.06	1
Live cells	95.54	1,168
Not labelled	2.39	29

Gate	%Gated	Cells/µL
All	100.00	1,223
Dead cells	2.86	35
Dead cells*	0.00	0
Live cells	94.56	1,156
Not labelled	2.58	32

Gate	%Gated	Cells/µL
All	100.00	1,233
Dead cells	4.40	54
Dead cells*	0.00	0
Live cells	93.55	1,154
Not labelled	2.05	25

Gate	%Gated	Cells/µL
All	100.00	218
Dead cells	6.72	15
Dead cells*	0.00	0
Live cells	87.47	190
Not labelled	5.80	13

Fig. 5 Exemplary cytograms (upper panel) and confocal images (lower panel) of *E. coli* (a-b) and *R. capsulatus* (c-d). Cells were suspended in nutrient-rich media and allowed to interact for 2 h with the controls (a, c) and blunt pillars (b, d). The cytograms are divided into four quadrants which divide cell populations: Lower Left – unlabeled cells; Lower Right – live cells (green fluorescence); Upper Right – dead and dying cells (green and red fluorescence at various ratios with the red arrow indicating nearly totally stained cells in red – for simplicity, all dead/dying cells were gated out together). The percentage of live and dead cell populations was determined as well as cell concentrations (see Tables below cytograms). Note that the concentrations were pre-diluted to allow reliable cell counting so that one cell passes through detection volume.

methods (cytometry and plates) and media used (Fig. 6a; *t* test: *p*-value <0.05, for details see Supplementary text 2). Here, cell plating yields significantly lower bactericidal efficiencies (BE) in rich medium (9%) than in PBS buffer (58%). Although the same aliquot of non-attached cells is used for cytometry and plating measurements, lower BE values measured by cytometry could be explained by cells counted as viable that may be in reality damaged without cell lysis (e.g., as in the antibacterial effect mediated by oxidative stress),[48] and hence unable to further proliferate on agar plates. Additionally, an experiment with *E. coli* in minimal medium (Fig. S4) revealed a similar trend to the behavior in rich medium, hence reinforcing the differences seen in the case of PBS. Similar BE values were determined by cytometry and microscopy, suggesting that for such structures, either method could be employed.
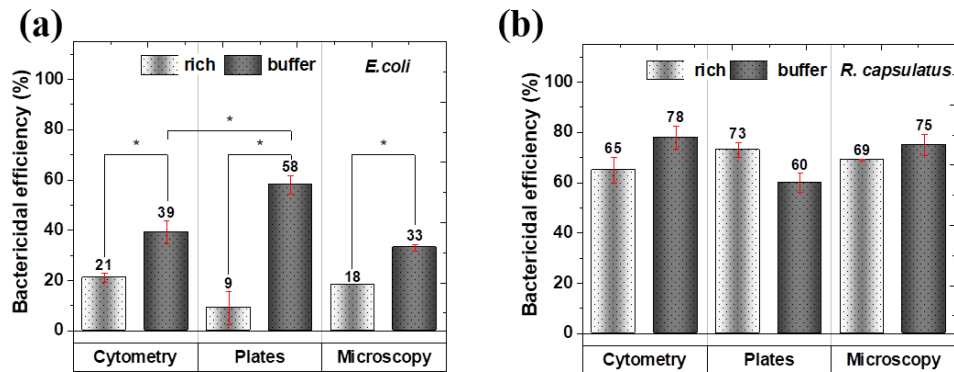

Fig. 6 Bactericidal efficiencies of etched silicon (L=390 nm, blunt tips) against (a) *E. coli* and (b) *R. capsulatus*. Bacteria were interacting with the surfaces for 2 h in rich medium and nutrient-free buffers. The BEs were determined based on number of viable cells remaining in solution, enumerated by plating method and flow cytometry (using live/dead fluorescent staining), according to Eq. 1 (see Methods for details). Additionally, BE was calculated based on the number of viable and non-viable cells attached on the surface by means of confocal microscopy and the live/dead staining using Eq. 2 (see Methods). The values are expressed as a mean ± SEM (n≥3 independent experiments). * p-value <0.05 refers to data that are significant.

Nanostructures with sharp pillars

We further focus on the activities of topographies with sharp pillars (Fig. 7). At the first glance, the killing efficiencies are higher when compared to the blunt pillars, likely due to sharp tips capable of impaling cells directly, hence killing faster. Overall, an ability to impale cells is debated in the field and future tests are required to provide further evidences. Note that the physical contact required to kill cells can be influenced not only by reducing the interaction volume but also by introducing dynamic conditions such as shaking or microfluidics.[49] However, although dynamic conditions may improve cell piercing, they may also prevent cell adhesion, which is the first step before cell deformation occurs. The BE values vary greatly for *E. coli* depending on the viability assay used (*t* test: *p*-value <0.001 for PBS) and they are always higher in PBS (Fig. 7a; *p*-value <0.05).

For example, the increases from 57% to 79% and from 29% to 55% were observed for plating and microscopy, respectively. The BEs derived from cytometry assays yielded lower values than the colony counting method, regardless of the media conditions, which is in contrast to observations with the blunt pillars, where a lower value was observed only in PBS. Although cytometry revealed a reduced number of viable cells, it did not show an accumulation of dead cells (Fig. S5).

In the case of *R. capsulatus* (Fig. 7b), the characteristics of non-adhering cells did not vary significantly, as observed for the other topography (Fig. 6b). For cells attached on the surface, BE was approximately three times lower for cells suspended in TBS (*p*-value <0.01). The origin of this difference is unclear, though extended incubation time (4 h) results in an increase to ~80% (Fig. S6) suggesting that perhaps a longer time for adhesion is required under these conditions. Overall, the data in Fig. S6 show that BE assessed by microscopy significantly increased over tested time, suggesting this method is likely more time-sensitive than the others.

Taken together, the two species tested reveal that various species can be differently affected by the environment. Moreover, while data obtained for *R. capsulatus* suggest that use of cytometry could potentially replace a more tedious and time-consuming plating method, the results for *E. coli* show discrepancies that cannot be corrected in a simple manner. However, it is evident that for a given condition the flow cytometry method enables high-throughput screening of bactericidal surface designs (with the ability to rapidly monitor killing rates and trajectories in nearly real-time), with further validation using the colony counting method. Overall, this opens an opportunity to advance the field at much faster rates.
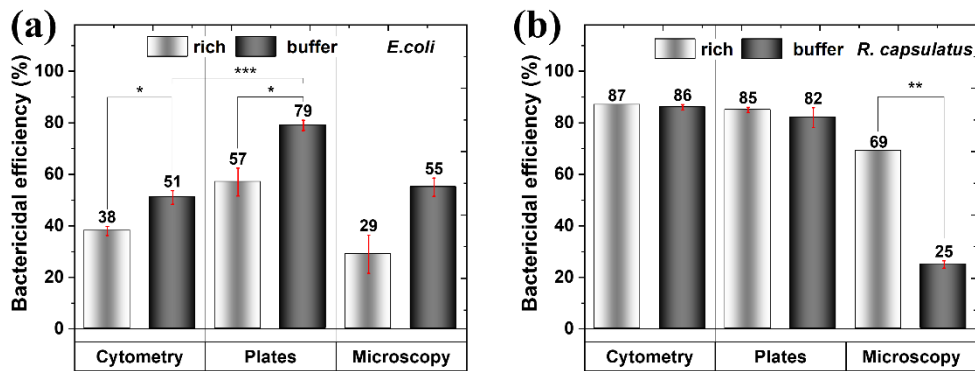
Fig. 7 Bactericidal efficiencies of etched silicon (L=3.6 μm, sharp tips) against (a) *E. coli* and (b) *R. capsulatus*. Bacteria were interacting with the surface for 2 h in rich medium and nutrient-free buffers. Bactericidal efficiencies were determined based on plating method, flow cytometry and microscopy. The values are expressed as a mean ± SEM (n ≥3 independent experiments). * p-value <0.05 refers to data that are significant; <0.01 very significant; <0.001 extremely significant.

New mechanistic insights

Since bactericidal efficiencies of sharp pillars against E. coli cells were greater when assessed by colony counting than by cytometry (Fig. 8a), we hypothesized that injured cells scored as live by cytometry could not recover and form colonies on plates. To probe this hypothesis, after the interaction with the surface and before plating, cells were allowed to recover in Super Optimal broth with Catabolite repression (SOC) for 30 min, a medium typically used to aid recovery of *E. coli* cells injured after exposure to an electrical pulse (electroporation; Fig. 8b-c). For the control surfaces, numbers of colonies were the same with and without incubation in SOC, indicating that there was no net growth during the recovery phase. When cells were exposed for 2 h to sharp pillars, we observed that incubation in SOC increased cell survival, leading to an average 19% decrease of BE values after recovery. Thus, the SOC treatment was sufficient to promote damage repair and survival in a fraction of cells, hence greatly reducing the differences observed between plating and flow cytometry. Remarkably, recovery in SOC did not help survival after exposure to sharp pillars for 4 h as the BE values remained the same. These findings imply that under favorable conditions bacteria can repair damages caused by nanostructured surfaces, and that there is likely a minimum time necessary to cause irreversible damage and cell death. Because the two bactericidal mechanisms differ significantly in killing rate, one should carefully consider the choice of the design to fit to the intended application.
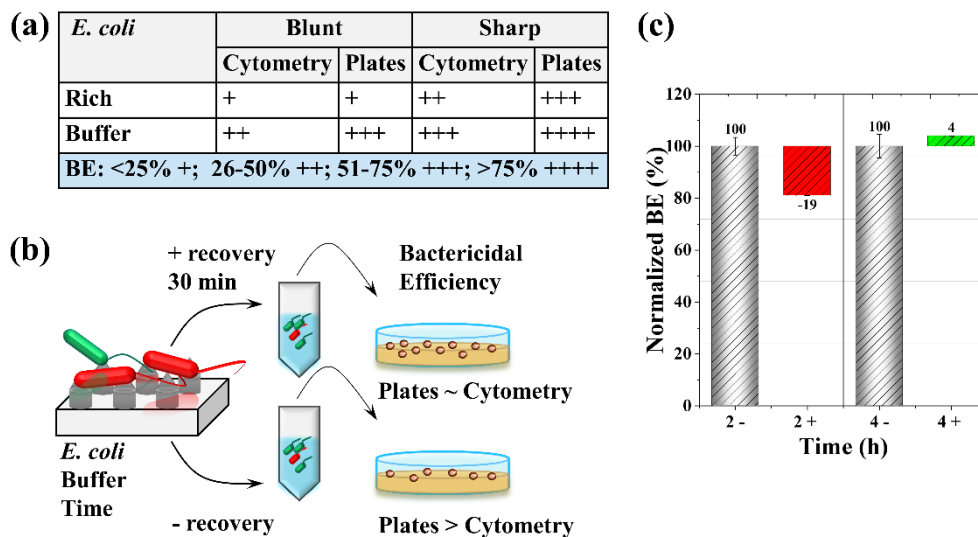

E. coli	Blunt		Sharp	
	Cytometry	Plates	Cytometry	Plates
Rich	+	+	++	+++
Buffer	++	+++	+++	++++
BE: <25% +; 26-50% ++; 51-75% +++; >75% ++++				

Fig. 8 The effect of recovery phase in SOC medium on bactericidal efficiency. (a) Table showing comparison between bactericidal efficiencies values of the blunt and sharp pillars to *E. coli* when tested in rich medium or PBS buffer. (b) Schematic presenting the outgrowth experiment setup and the effect on the number of colonies. (c) Normalized BEs of silicon with sharp pillars against *E.coli* in PBS buffer interacting with the surfaces for 2 and 4 h, with (+) and without (-) 30 min of the recovery phase. Red and green colors refer to decrease and increase, respectively. The values are expressed as a mean ± SEM (n = 5

Conclusions

The field of bioinspired nanostructured surfaces with antimicrobial properties is rapidly growing as an attractive alternative to the existing chemical approaches to manage microbial contamination. Unfortunately, as the material designs advance, it becomes more complex to objectively compare competing technologies due to the lack of standard approaches for testing their performances. Generally, many approaches can be correct as long as they inform the ultimate application. However, some standard testing conditions are needed to facilitate direct comparison between new technologies, which ideally, should be further expanded to reveal and verify the true potency and utility of the material. Since the materials kill upon contact, here, we stress the need to characterize cells that are both unattached and attached on the surface. We also show the importance of medium selection and how the ultimate results can be strongly affected by this choice. Despite the fact that the plating method is a gold standard to monitor growth and is ubiquitous in every laboratory setting, we show how flow cytometry can become a new valuable method to advance the field. Not only can it accelerate the material development (giving feedback on materials and process designs in minutes and not days) but it can also add to the mechanistic understanding of how these new surfaces operate.

Materials and Methods

Fabrication of nanostructured surfaces

Two nanostructured surfaces were fabricated that possess nanopillars with either blunt (wide tip) or sharp (narrow tip), according to the process we have recently developed.[18] Briefly, silicon wafers (4", p-type boron-doped, <100>, resistivity 10-20 $\Omega \cdot cm^{-1}$, 525 ± 25 μm, purchased from Silicon Valley Microelectronics, Inc.) were cleaned with acetone and isopropanol (IPA). Subsequently, reactive ion etching (RIE) was conducted using O_2/SF_6 plasma (Oxford PlasmaLab 100) with the following conditions: 200 W RF power, 20 °C temperature, 35 mTorr pressure, 36 O_2 and 40 SF_6 sccm flows, for 1.5 and 15 min (blunt and sharp pillars, respectively). The etched samples were cut into 1 cm^2 and sterilized using 70% ethanol prior to use in further experiments. Note, the sample size by industrial standard is set to a square of 50 mm and it is reduced here below the limits. However, it follows the guidance set by the vast range of literature and allows to accommodate a large number of samples required for biological and technical replicates, given a currently limited scalability of fabrication, which mainly relies on reactive ion etching.

Characterization of the nanostructured surfaces

The topographical features such as pillar height, base diameter, density (number of pillars per surface area), and pitch (pillar center-to-center distance) were determined based on Scanning Electron Microscopy (SEM) images. Micrographs were taken using a JEOL 7500 Field Emission SEM, operating at 15 kV. The ImageJ software[50] was used for image analysis. At least five independent fields were measured. The pitch was quantified using a nearest-neighbor-distances (NND) ImageJ plugin (https://icme.hpc.msstate.edu Author: Yuxiong Mao).

The surface wettability was characterized by a measurement of static contact angle of water (5 μl) at room temperature by means of Drop Shape Analyzer (KRÜSS GmbH, Germany).

Media preparation and cell cultures

For media recipes please refer to Supporting Information.

Two Gram-negative bacteria *Escherichia* (*E.*) *coli* and *Rhodobacter* (*R.*) *capsulatus* were used in this study. Bacterial stocks were maintained frozen at -70°C and cultured on LB medium (*E. coli* strain DH5α) and [S]RCVPY medium (*R. capsulatus* strain U43[pBBR1MCS-2]),[51] supplemented with kanamycin (30 μg/ml). To prepare the inoculum for application to the materials, *E. coli* was cultured to mid-exponential phase (optical density at 600 nm, OD_{600} ~0.6) in LB medium, aerobically, at 37 °C and with shaking at 250 rpm. *R. capsulatus* was similarly cultured but in [S]RCVPY medium with kanamycin, under semi-aerobic, chemoheterotrophic conditions in the dark (silicone sponge closures), at 33 °C and with shaking at 125 rpm. The bacteria were recovered by centrifugation, washed twice, and diluted into fresh media [rich or minimal (MR26 and M9 with glucose)] or nutrient-free buffers [phosphate-buffered saline (PBS), Tris-buffered saline (TBS), and M9 salts] to the concentration of 5 x 10^7 colony forming units (cfu)/ml.

Antibacterial properties of the nanostructured surfaces

The antimicrobial properties of nanostructured surfaces were quantitatively evaluated using the adhesion based-assay which relies on: (1) adding an inoculum (here, droplet of V=20 µl) onto the surface (test and control), (2) incubation, (3) rinsing and collecting non-attached cells, and (4) assessing cell viability of non-attached cells and cells attached on the surface. To assess the viability, various techniques were employed and compared (sections 1-3).

In details, a 24-well protein crystallization plate containing a pedestal located centrally in a well (Chryschem, Hampton Research) was used as a humidity-controlled experimental system to prevent evaporation. To assure even humidity, 1 ml of sterile water was added to each well, the nanostructured surface or control was placed on the top of pedestal, the inoculum was added, and the well was sealed with vacuum grease and a glass cover slide (22 mm diameter). All experiments were performed at room temperature (RT, 25 ± 0.5 °C) up to 4 h. Alternatively, samples can be placed in a petri dish equipped with a filter paper moisten with 1 ml of sterile water, positioned on a microscope slide lifted on toothpicks from the filter.

The Colony Counting Method (section 1) and flow cytometry (section 2) were used as viability tests to analyze non-adhering bacteria. The reduction in viability induced by the surface exposure was calculated as Bactericidal Efficiency (BE) according to the following equation: $BE = 100 - \left(\frac{V_x}{V_{ctrl}}\right) \cdot 100 \ (Eq. 1)$, where V refers to number of viable cells, x – experimental sample, and $ctrl$ – control sample.

The viability of attached bacteria onto the surfaces were investigated by confocal microscopy of live/dead stained cells (section 3). Here, BE was calculated based on number of Viable (V) and Non-Viable (NV) cells attached on the surface using the following equation: $BE = \left(\frac{NV_x}{V_x + NV_x}\right) \cdot 100 \ (Eq. 2)$. It was assumed that BE for the controls is 0%.

1. Colony counting method

At given time intervals, non-attached cells were retrieved from control and tested surfaces by rinsing with fresh medium (rinsing = mixing 10 times with 20 µl of medium by pipette, yielding 2 x dilution), and serially diluted further to obtain 30-300 colonies per plate. Cell suspensions (50 µl) were plated on rich medium containing appropriate antibiotics when necessary. Finally, colonies were counted, and BE was determined.

Glass cover slides were chosen as routine controls as bacterial growth on these surfaces was found invariant to non-etched (smooth) silicon wafers.[18] A range of numbers of mixing by pipetting (5-50) was tested to elucidate a potential impact on BE, as well as rinsing with an increased volume (500 µl). In both cases, no significant differences were found (data not shown).

2. Flow cytometry assay

The same retrieved cells (section 1) were also diluted with 1 x TBS to appropriate concentrations, necessary for reliable counting using flow cytometer (CytoFLEX, Beckman Coulter Life Sciences). Subsequently, the cells were stained with LIVE/DEAD® BacLight™ Bacterial Viability Kit (L7012, Invitrogen) per instructions. The kit contains SYTO 9 (green) and propidium iodide (PI, red) dyes that counterstain the cells based on their membrane integrity. Bacterial cells with intact membranes are stained green, whereas cells with a damaged membrane (that are considered to be dead or injured) are stained red, or red and green. Please see Figs S1-3 for details about optimization of instrumental setup. After 15 min of incubation in the dark, cells were analyzed using flow cytometer with 96-well plate loader. The cells were excited with 488 nm and 561 nm lasers and the emission of SYTO9 and PI were detected using 525/40 and 610/20 bandpass filters, respectively. 10,000 events were collected per sample. Flow rates of 10 µl/min were utilized. The number of cells per µl was derived after appropriate gating.

The same instrumental setup was used to monitor *E. coli* and *R. capsulatus* cells susceptibility (compatibility) to various media. Cells grown to mid-log phase were harvested and resuspended in five media: MR26, M9 with glucose, M9 (salts), TBS and PBS. The suspensions were stained with BacLight™ kit at time intervals (from 0 to 20 hours), incubated for 15 min in a dark, and examined by flow cytometry. The total number of the cells and population of dead cells (% of total number of cells) were analyzed.

3. Confocal imaging

The viability of the cells that remained attached onto the tested surfaces was evaluated by live/dead staining and confocal microscopy. At given time intervals, after the surfaces were washed and non-adhering cells collected, they were additionally rinsed with 1 x TBS to remove traces of medium (known to quench the fluorophores), followed by staining with the live/dead kit per instructions. Image

acquisition and analysis were performed using a Nikon Eclipse Ti microscope with 100x objective, a 1.45 oil immersion lens, and NIS-Elements AR 4.50.00 software. The cells were visualized by using 470 and 555 nm excitations and 515/30 and 595/40 emission filters. Two color channels, green and red, were acquired for each image. To remove the fluorescent background noise from the image, brightness levels in every channel were adjusted.

Recovery from cell damage

An additional experiment was performed to evaluate whether the cells that interacted with nanostructures can repair damages and recover viability. *E. coli* cells were interacting with sharp pillars in PBS medium for 2 and 4 h, followed by rinsing, and viable cells were quantified by plating and flow cytometry. An aliquot of the cells was diluted with super optimal broth with catabolite repression medium (SOC) and outgrown at 37 °C, 250 rpm, for 30 min. Cells (50 µl) were plated on rich medium and number of colonies counted.

Statistical analysis

Please see Supporting Information.

Author Contributions

The manuscript was written through contributions of all authors. All authors have given approval to the final version of the manuscript.

Conflicts of interest

There are no conflicts to declare.

Acknowledgements

Notes and references

1   Y. Cheng, G. Feng and C. I. Moraru, *Front. Microbiol.*, 2019, **10**, 1–17.

2   C. Adlhart, J. Verran, N. F. Azevedo, H. Olmez, M. M. Keinänen-Toivola, I. Gouveia, L. F. Melo and F. Crijns, *J. Hosp. Infect.*, 2018, **99**, 239–249.

3   N. Encinas, C.-Y. Yang, F. Geyer, A. Kaltbeitzel, P. Baumli, J. Reinholz, V. Mailänder, H.-J. Butt and D. Vollmer, *ACS Appl. Mater. Interfaces*, 2020, **12**, 21192–21200.

4   J. A. Callow and M. E. Callow, *Nat. Commun.*, 2011, **2**, 244.

5   V. T. H. Pham, V. K. Truong, A. Orlowska, S. Ghanaati, M. Barbeck, P. Booms, A. J. Fulcher, C. M. Bhadra, R. Buividas, V. Baulin, C. J. Kirkpatrick, P. Doran, D. E. Mainwaring, S. Juodkazis, R. J. Crawford and E. P. Ivanova, *ACS Appl. Mater. Interfaces*, 2016, **8**, 22025–22031.

6   D. P. Linklater, V. A. Baulin, S. Juodkazis, R. J. Crawford, P. Stoodley and E. P. Ivanova, *Nat. Rev. Microbiol.*, 2021, **19**, 8–22.

7   Centers for Disease Control and Prevention, *Antibiotic resistance threats in the United States, 2019*, Atlanta, Georgia, 2019.

8   S. H. Nguyen, H. K. Webb, P. J. Mahon, R. J. Crawford and E. P. Ivanova, *Molecules*, 2014, **19**, 13614–13630.

9   D. P. Linklater, S. Juodkazis and E. P. Ivanova, *Nanoscale*, 2017, **9**, 16564–16585.

10   J. Hasan, S. Jain and K. Chatterjee, *Sci. Rep.*, 2017, **7**, 41118.

11   V. Narasimhan, R. H. Siddique, J. O. Lee, S. Kumar, B. Ndjamen, J. Du, N. Hong, D. Sretavan and H. Choo, *Nat. Nanotechnol.*, 2018, **13**, 512–519.

12   A. Tripathy, P. Sen, B. Su and W. H. Briscoe, *Adv. Colloid Interface Sci.*, 2017, **248**, 85–104.

13   R. Jiang, L. Hao, L. Song, L. Tian, Y. Fan, J. Zhao, C. Liu, W. Ming and L. Ren, *Chem. Eng. J.*, 2020, **398**, 125609.

14   Q. Cui, T. Liu, X. Li, K. Song and D. Ge, *ACS Appl. Nano Mater.*, 2020, **3**, 4599–4609.

15   C. D. Bandara, S. Singh, I. O. Afara, A. Wolff, T. Tesfamichael, K. Ostrikov and A. Oloyede, *ACS Appl. Mater. Interfaces*, 2017, **9**, 6746–6760.

16   E. P. Ivanova, J. Hasan, H. K. Webb, V. K. Truong, G. S. Watson, J. A. Watson, V. A. Baulin, S. Pogodin, J. Y. Wang, M. J. Tobin, C. Lobbe and R. J. Crawford, *Small*, 2012, **8**, 2489–2494.

17   E. P. Ivanova, D. P. Linklater, M. Werner, V. A. Baulin, X. Xu, N. Vrancken, S. Rubanov, E. Hanssen, J. Wandiyanto, V. K. Truong, A. Elbourne, S. Maclaughlin, S. Juodkazis and R. J. Crawford, *Proc. Natl. Acad. Sci.*, 2020, **117**, 12598–12605.

18   M. Michalska, F. Gambacorta, R. Divan, I. S. Aranson, A. Sokolov, P. Noirot and P. D. Laible, *Nanoscale*, 2018, **10**, 6639–6650.

19   D. P. Linklater, M. De Volder, V. A. Baulin, M. Werner, S. Jessl, M. Golozar, L. Maggini, S. Rubanov, E. Hanssen, S. Juodkazis and E. P. Ivanova, *ACS Nano*, 2018, **12**, 6657–6667.

20   S. Pogodin, J. Hasan, V. A. Baulin, H. K. Webb, V. K. Truong, T. H. Phong Nguyen, V. Boshkovikj, C. J. Fluke, G. S. Watson, J. A. Watson, R. J. Crawford and E. P. Ivanova, *Biophys. J.*, 2013, **104**, 835–840.

21   E. P. Ivanova, J. Hasan, H. K. Webb, G. Gervinskas, S. Juodkazis, V. K. Truong, A. H. F. Wu, R. N. Lamb, V. A. Baulin, G. S. Watson, J. A. Watson, D. E. Mainwaring and R. J. Crawford, *Nat. Commun.*, 2013, **4**, 2838.

22   M. N. Dickson, E. I. Liang, L. A. Rodriguez, N. Vollereaux and A. F. Yee, *Biointerphases*, 2015, **10**, 021010.

23   T. S. Heckmann and J. D. Schiffman, *ACS Appl. Nano Mater.*, 2020, **3**, 977–984.

24   S. M. Kelleher, O. Habimana, J. Lawler, B. O' Reilly, S. Daniels, E. Casey and A. Cowley, *ACS Appl. Mater. Interfaces*, 2016, **8**, 14966–14974.

25   P. Zhang, L. Lin, D. Zang, X. Guo and M. Liu, *Small*, 2017, **13**, 1–9.

26   M. J. Hancock, K. Sekeroglu and M. C. Demirel, *Adv. Funct. Mater.*, 2012, **22**, 2223–2234.

27   S. M. Imani, R. Maclachlan, K. Rachwalski, Y. Chan, B. Lee, M. McInnes, K. Grandfield, E. D. Brown, T. F. Didar and L. Soleymani, *ACS Nano*, 2020, **14**, 454–465.

28   M. van de Lagemaat, A. Grotenhuis, B. van de Belt-Gritter, S. Roest, T. J. A. Loontjens, H. J. Busscher, H. C. van der Mei and Y. Ren, *Acta Biomater.*, 2017, **59**, 139–147.

29   M. D. Campos, P. C. Zucchi, A. Phung, S. N. Leonard and E. B. Hirsch, *PLoS One*, 2016, **11**, e0160728.

30   S. W. M. A. I. Senevirathne, J. Hasan, A. Mathew, M. Woodruff and P. K. D. V. Yarlagadda, *RSC Adv.*, 2021, **11**, 1883–1900.

31   J. Sjollema, S. A. J. Zaat, V. Fontaine, M. Ramstedt, R. Luginbuehl, K. Thevissen, J. Li, H. C. van der Mei and H. J. Busscher, *Acta Biomater.*, 2018, **70**, 12–24.

32   R. Kaur and S. Liu, *Prog. Surf. Sci.*, 2016, **91**, 136–153.

33   M. Katsikogianni and Y. Missirlis, *Eur. Cells Mater.*, 2004, **8**, 37–57.

34   A. Valiei, N. Lin, J.-F. Bryche, G. McKay, M. Canva, P. G. Charette, D. Nguyen, C. Moraes and N. Tufenkji, *Nano Lett.*, 2020, **20**, 5720–5727.

35   C. Davis, *J. Microbiol. Methods*, 2014, **103**, 9–17.

36   P. Stiefel, S. Schmidt-Emrich, K. Maniura-Weber and Q. Ren, *BMC Microbiol.*, 2015, **15**, 1–9.

37   F. Hammes, M. Berney and T. Egli, in *High Resolution Microbial Single Cell Analytics*, eds. S. Müller and T. Bley, Springer Berlin Heidelberg, Berlin, Heidelberg, 2011, pp. 123–150.

38   J. T. Seil and T. J. Webster, *Int. J. Nanomedicine*, 2012, **7**, 2767–2781.

39   A. Elbourne, R. J. Crawford and E. P. Ivanova, *J. Colloid Interface Sci.*, 2017, **508**, 603–616.

40   M. T. Cabeen and C. Jacobs-Wagner, *Nat. Rev. Microbiol.*, 2005, **3**, 601–610.

41   M. Köller, N. Ziegler, C. Sengstock, T. A. Schildhauer and A. Ludwig, *Biomed. Phys. Eng. Express*, 2018, **4**, 055002.

42   S. Wu, F. Zuber, K. Maniura-Weber, J. Brugger and Q. Ren, *J. Nanobiotechnology*, 2018, **16**, 20.

43   Y. Xie, X. Qu, J. Li, D. Li, W. Wei, D. Hui, Q. Zhang, F. Meng, H. Yin, X. Xu, Y. Wang, L. Wang and Z. Zhou, *Sci. Total Environ.*, 2020, **738**, 139714.

44   *Japanese Industrial Standard JIS Z 2801:2010, Antibacterial products - Test for antibacterial activity and efficacy*, Japanese Standards Association, Tokyo, Japan, 2010.

45   C. Trappetti, L. Gualdi, L. Di Meola, P. Jain, C. C. Korir, P. Edmonds, F. Iannelli, S. Ricci, G. Pozzi and M. R. Oggioni, *BMC Microbiol.*, 2011, **11**, 75.

46   C. Signas, G. Raucci, K. Jonsson, P. E. Lindgren, G. M. Anantharamaiah, M. Hook and M. Lindberg, *Proc. Natl. Acad. Sci.*, 1989, **86**, 699–703.

47   K. Jindai, K. Nakade, K. Masuda, T. Sagawa, H. Kojima, T. Shimizu, S. Shingubara and T. Ito, *RSC Adv.*, 2020, **10**, 5673–5680.

48   J. Jenkins, J. Mantell, C. Neal, A. Gholinia, P. Verkade, A. H. Nobbs and B. Su, *Nat. Commun.*, 2020, **11**, 1626.

49   T. Diu, N. Faruqui, T. Sjöström, B. Lamarre, H. F. Jenkinson, B. Su and M. G. Ryadnov, *Sci. Rep.*, 2014, **4**, 7122.

50   C. a Schneider, W. S. Rasband and K. W. Eliceiri, *Nat. Methods*, 2012, **9**, 671–675.

51   C. Kirmaier, P. D. Laible, K. Czarnecki, A. N. Hata, D. K. Hanson, D. F. Bocian and D. Holten, *J. Phys. Chem. B*, 2002,

106, 1799–1808.

52   P. D. Laible, A. N. Hata, A. E. Crawford and D. K. Hanson, *J. Struct. Funct. Genomics*, 2005, **6**, 95–102.